Cyclopropanation reactions catalysed by dendrimers possessing one metalloporphyrin active site at the core: linear and sigmoidal kinetic behaviour for different dendrimer generations

Petr Vinš, Abel de Cózar, Iván Rivilla, Kateřina Nováková, Ronen Zangi, Josef Cvačka, Iosune Arrastia, Ana Arrieta, Pavel Drašar, José I. Miranda, Fernando P. Cossío

PII: S0040-4020(16)30013-8
DOI: 10.1016/j.tet.2016.01.013
Reference: TET 27420

To appear in: *Tetrahedron*

Received Date: 28 July 2015
Revised Date: 9 December 2015
Accepted Date: 7 January 2016

Please cite this article as: Vinš P, de Cózar A, Rivilla I, Nováková K, Zangi R, Cvačka J, Arrastia I, Arrieta A, Drašar P, Miranda JI, Cossío FP, Cyclopropanation reactions catalysed by dendrimers possessing one metalloporphyrin active site at the core: linear and sigmoidal kinetic behaviour for different dendrimer generations, *Tetrahedron* (2016), doi: 10.1016/j.tet.2016.01.013.

Cyclopropanation reactions catalysed by dendrimers possessing one metalloporphyrin active site at the core: linear and sigmoidal kinetic behaviour for different dendrimer generations

Petr Vinš,[a] Abel de Cózar,[bcd] Iván Rivilla,[b] Kateřina Nováková,[e] Ronen Zangi,[bc] Josef Cvačka,[e] Iosune Arrastia,[bd] Ana Arrieta,[b] Pavel Drašar[a], José I. Miranda,[f] and Fernando P. Cossío*[bd]

Graphical Abstract:

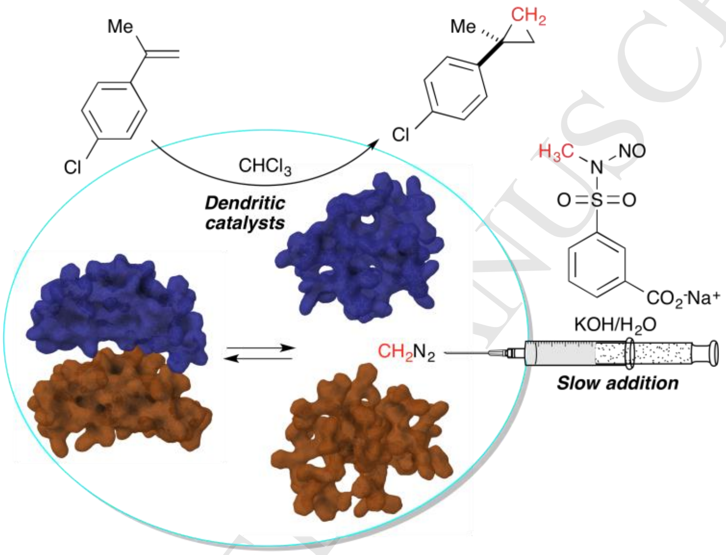

Abstract: Experimental and computational studies on dendrimers possessing a Fe(porphyrin) catalytic core and polyether dendritic arms show that these macromolecules promote efficiently the (2+1) cycloaddition between a model alkene

---

[a] *University of Chemistry and Technology in Prague, Department of Chemistry of Natural Compounds, Technická 5, 16628 Prague 6, Czech Republic*
[b] *Departamento de Química Orgánica I, and Centro de Innovación en Química Avanzada (ORFEO-CINQA), Universidad del País Vasco / Euskal Herriko Unibertsitatea (UPV/EHU), Pº Manuel Lardizabal 3, 20018 San Sebastián / Donostia, Spain*
[c] *Ikerbasque, Basque Foundation for Science, 48013, Bilbao, Spain*
[d] *Donostia International Physics Center (DIPC), Pº Manuel Lardizabal, 20018, San Sebastián / Donostia, Spain*
[e] *Institute of Organic Chemistry and Biochemistry AS CR, v.v.i., Flemingovo nám. 2, 16610 Prague 6, Czech Republic*
[f] *SGIker, NMR Facility, Universidad del País Vasco / Euskal Herriko Unibertsitatea (UPV/EHU), Pº Manuel Lardizabal 3, 20018 San Sebastián / Donostia, Spain*
* Corresponding author. Tel. +34 943 015442; fax: +34 943 015270; e-mail: fp.cossio@ehu.es

and diazomethane. The reaction is kinetically efficient and competitive with smaller catalysts. Lower generations of dendrimers exhibit a normal hyperbolic kinetic behaviour, whereas third- and fourth-generation dendrimers show a sigmoidal kinetic profile, compatible with cooperative effects most likely due to aggregation phenomena. This behaviour resembles that observed for Fe(porphyrin) containing biomolecules such as cytochromes and haemoglobin.

Introduction

Catalytic dendrimers[1] constitute an active research field, which has been intensively studied in the past two decades. These efforts have resulted in the development of novel catalysts possessing one metallic centre[2] and well-defined macromolecular organocatalysts.[3] These macromolecular entities possess several interesting properties in homogeneous catalysis such as easier catalyst recovery by precipitation[4] or nano- and ultrafiltration.[5] Despite the fact that the separation of catalysts immobilized on solid supports will remain easier, there are other advantages of the dendritic approach. For example, higher overall activities of the homogenous systems, uniformity of catalyst structure and also the possibility of higher catalyst loading in the case of dendrimers with catalytic sites on the peripheries or branching points.

Installing a catalytic site onto a dendritic moiety either at the core or at the periphery can result in distinct catalytic properties with respect to polymeric or small molecule analogues. This variation has been termed as a “dendrimer effect”.[6] In the case of core-functionalized dendrimers, the growth of the structure can enhance the catalytic performance by creation of tailored microenvironment in its centre. But also it can reduce the efficiency of the catalyst by rendering the central function hardly accessible for the substrate. Such activity decrease can be either successive,[7] or also abrupt, showing very similar behaviour for lower generations and swift downturn after a trespass of certain molecule size limit[8]. Quantitative measurements of dendrimer catalyst activity in dependence on the generation number are not very frequent; however, there are several examples of such studies,[9,10] showing different effects coming from dendron size to catalytic performance.

In previous work, we studied dendrimers with one active site[10, 11] or one fluorophore[12] at the core. We observed negative, i.e., non-cooperative dendrimer effects with increasingly high generation numbers. Moreover, Morandi and Carreira[13] have recently published a very interesting study on the cyclopropanation of alkenes.

We thought that this formal (2+1) cycloaddition [14] involving very reactive intermediates and relatively small substrates could be an interesting system to observe dendrimer effects in which the steric hindrance of the dendritic catalysts could be less relevant than in previously studied reactions.

According to the Morandi-Carreira approach, the cyclopropanation of various styrene derivatives is performed in 6 M KOH in an open vial, with continuous addition of a water soluble diazomethane precursor, which provides this reactive intermediate under basic conditions, and under catalysis by Fe(III) tetraphenylporphyrin chloride (Fe(TPP)Cl) complex. [15] The approach successfully avoided hazardous isolation and handling of diazomethane.[16]

Within the context established by the precedents discussed above, in this paper we present our results on the dendrocatalytic version of the Morandi-Carreira reaction. In particular, we will focus our research on the catalytic behaviour of different generations of dendritic porphyrin-based[17] catalysts in order to assess the possibility of finding emergent properties for higher generations of these macromolecules.

Results and discussion

Synthesis of catalytic dendrimers. The general procedure followed for the synthesis of the catalysts is shown in Scheme 1 and was based on convergent strategy[18] for the synthesis of dendrimers. Thus, Fréchet-type disubstituted benzyloxy dendrons were prepared first up to the fourth generation. These dendritic wedges were obtained in the form of bromides (Br-D_n, n=1-4, see Scheme 1) following the original procedure.[19]

Subsequent conjugation of bromides Br-D_n with 5,10,15,20-tetrakis(4-hydroxyphenyl)porphyrin (TPP-$(OH)_4$, **1**) was carried out under conventional Williamson etherification conditions using K_2CO_3 as base and DMF as solvent, to yield dendrimeric porphyrins **2c-f** (generations **G1-G4**, see Scheme 1). Lower-weight analogous porphyrins tetrakis(4-methoxyphenyl)porphyrin **2a** and tetrakis(4-benzyloxyphenyl)porphyrin **2b** (0th generation dendrimer **G0**) were prepared for the shake of completeness and continuity using methyl iodide and benzyl bromide as Williamson electrophiles, respectively. Metallated porphyrins **3a-f** including dendrimer generations **G'0-G'4** were obtained by addition of ferrous chloride to porphyrins **2a-f** in refluxing solution of THF. Under these reaction conditions, Fe(II) intermediates were exposed to air and therefore the corresponding Fe(III)Cl-porphyrin derivatives[20] were obtained as stable compounds. Metallated porphyrins **3a-f** were characterized by HRMS (compounds **3a-c**) or by MALDI-TOF-MS (dendrimers **3d-f**) as well as by UV-Visible spectroscopy. Non-metallated precursors **2a-f** were analysed by ^{1}H-NMR and ^{13}C-NMR spectroscopy (see the Experimental Section and the Supplementary data for further details).

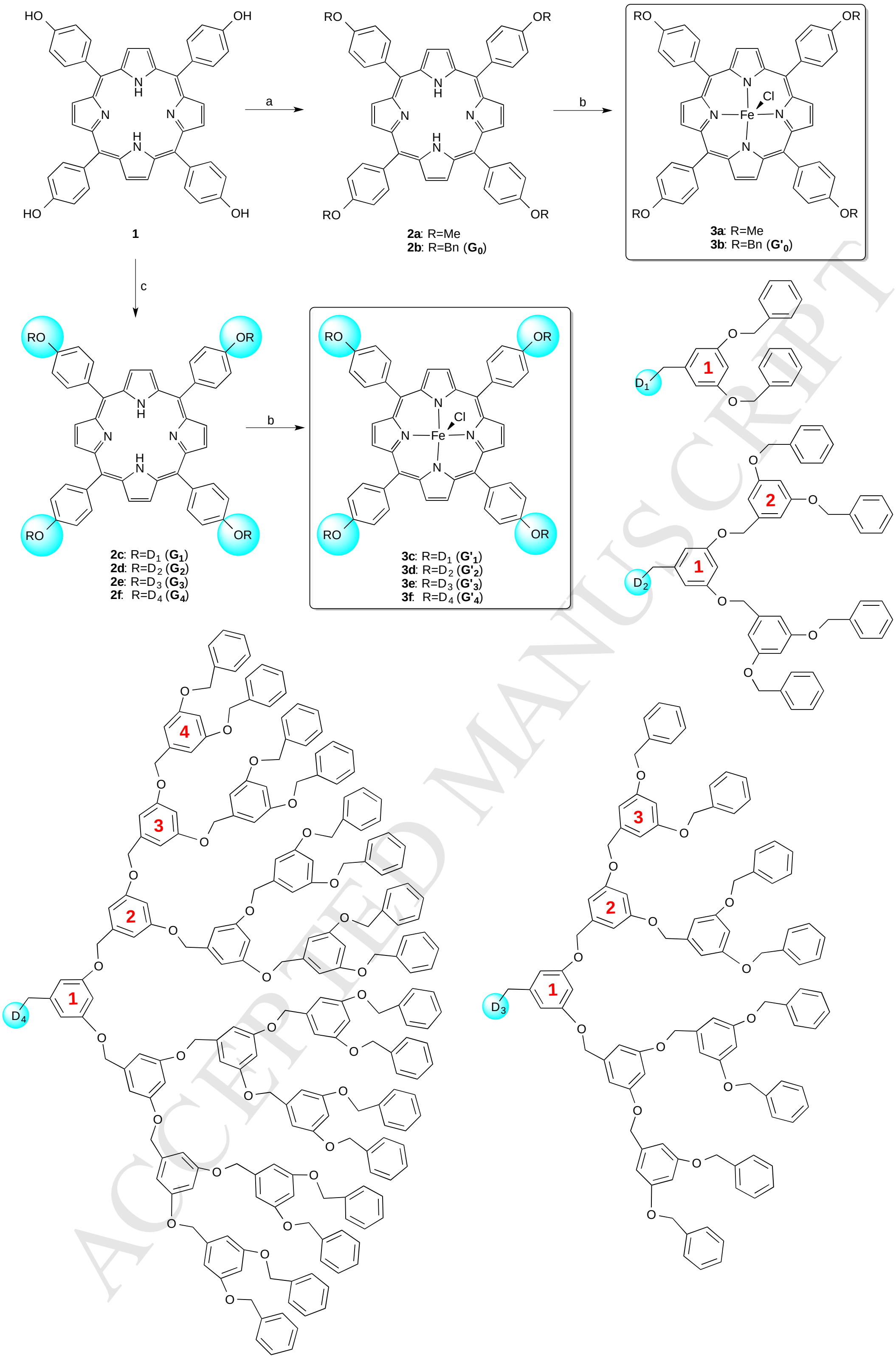

Scheme 1. Synthesis of dendrimeric catalysts **3a-f**. Reagents and conditions: a) K_2CO_3, DMF, MeI (for **2a**) or BnBr (for **2b**); b) $FeCl_2$, THF, O_2 (air); c) K_2CO_3, DMF, Br-D_n (n=1-4).

Catalytic properties. Once we had prepared compounds **3a-f**, we studied their behaviour as catalysts in the cyclopropanation of substituted styrene **4** (1-chloro-4-(prop-1-en-2-yl)benzene) with diazomethane in deuterated chloroform. Following the Morandi-Carreira procedure,[13] diazomethane was generated in situ from 3-(*N*-methyl-*N*-nitrososulfamoyl)benzoate **6** (Scheme 2). The reaction mixtures were analysed by ^{1}H-NMR using 1,2,3-trimethoxybenzene (TMB) as internal standard for the integration of the appropriate diagnostic signals corresponding to the internal standard, the reactant **4** and the (2+1) cycloadduct 1-(4-chlorophenyl)-1-methylcyclopropane **5** (Figure 1).

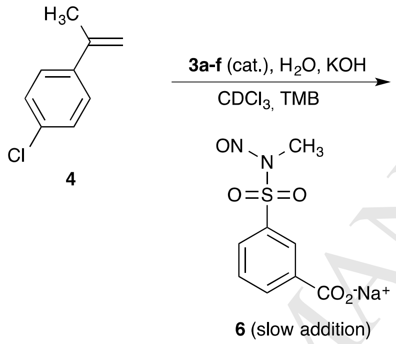

Scheme 2. Cyclopropanation of styrene **4** (1-chloro-4-(prop-1-en-2-yl)benzene) with sodium 3-(*N*-methyl-*N*-nitrososulfamoyl)benzoate **6** catalysed by metalloporphyrins **3a-f**. TMB: 1,2,3-trimethoxybenzene.

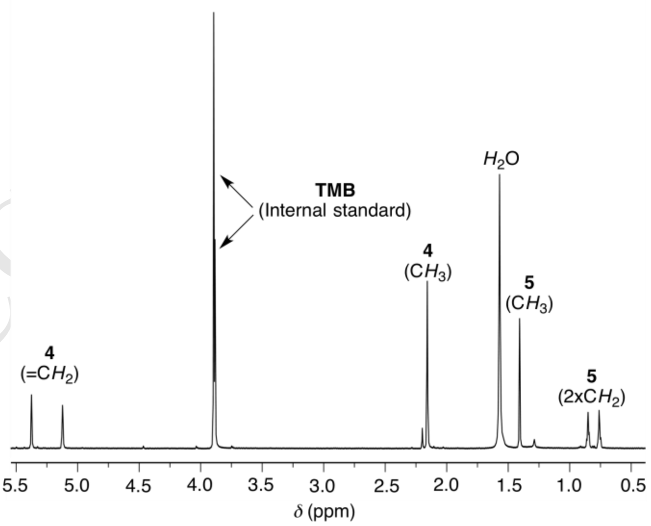

Figure 1. Example of ^{1}H-NMR spectrum recorded for the reaction between styrene **4** and *in situ* generated diazomethane to yield cyclopropane derivative **5** in the presence of catalyst **3b** (**G'$_0$**, 2 mol %) at room temperature and after a reaction time of 40 min. TMB: 1,2,3-trimethoxybenzene.

According to the mechanism accepted for this kind of reactions, precursor **6** generates one equivalent of diazomethane in a solution of KOH in water (Scheme 3) with the concomitant formation of highly polar salt **7**, which remains in the aqueous phase. *In situ* formed diazomethane passes to the organic phase and reacts with the catalytic metalloporphyrin **3'** to yield the corresponding carbene-Fe complex. It has been proposed that reactive and unstable Fe(II) species are the actual active catalysts.[21] Indeed, it has been suggested[21a,c] that the diazomethane reactant can reduce the Fe(III)Cl complex **3** to the corresponding Fe(II) derivative **3'**. In addition, the Fe-carbene intermediate can exist in at least two different spin states as a bridged complex.[22] denoted as **A** in Scheme 3, which is in equilibrium with the corresponding axial isomer **B**. This latter intermediate interacts with the alkene to yield the (2+1) cycloadduct **5**, with the concomitant release of porphyrin **3'**, thus completing the catalytic cycle.

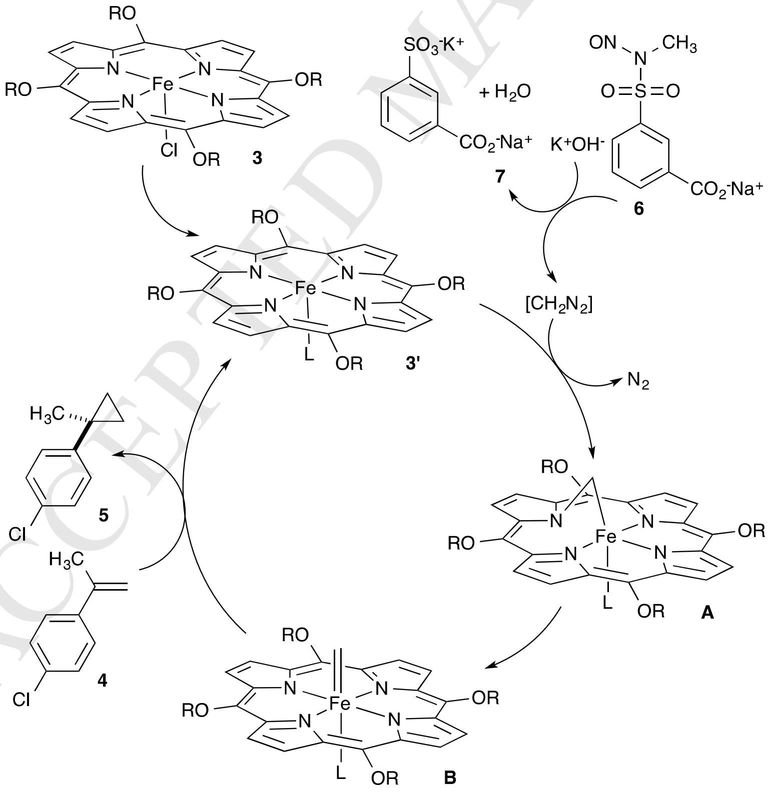

Scheme 3. Catalytic cycle for the cyclopropanation of alkene **4** to yield cyclopropane **5** in the presence of diazomethane precursor **6** and metalloporphyrins **3**.

The reaction was performed in a biphasic system (water/$CDCl_3$).[13] Using this approach, hydrophobic catalyst and substrate were dissolved in a small quantity of chloroform, which was vigorously stirred together with an aqueous solution of KOH. The reaction vessel was a flask that permitted a flow-off of excessive gas phase during the addition process through injected needle. Compound **6** was slowly added into the reaction system by means of an automatic syringe, providing diazomethane under basic conditions. *In situ* generated diazomethane participated in the cyclopropanation reaction after its phase transfer into the droplets of chloroform. In the organic phase it was consumed by the metalloporphyrin catalyst **3** to form the corresponding metal-carbene intermediate, which reacted with the styrene substrate **4**. Due to the slow addition of **6**, diazomethane was present in the reaction system in substoichiometric quantity. On the contrary, the substrate in the organic phase was in local excess.

Since Morandi and Carreira[13] used a 2 mol % of Fe(TTP)Cl catalyst in the original work, we started our study on dendrimeric analogues by testing the **4**→**5** reaction with loadings of 1-10 mol % of Fe(TPP)Cl at an addition rate of 1 eq. of Fe(TTP)Cl per hour (Figure 2). Experiments with 1, 2, and 4 mol % barely differed, while the experiment with 10 mol % showed lower performance (Figure 2). This indicates that catalyst loads of 1-2 mol % were able to process the incoming diazomethane at very similar rate. Since precursor **6** and diazomethane were in a low ratio with respect to the substrate, higher catalyst loadings did not accelerate the reaction. However, consumption of substrate **4** took place at a rate lower than that associated with the instantaneous conversion of **6** into diazomethane and subsequent cyclopropanation of alkene **4** to form cyclopropane derivative **5**.

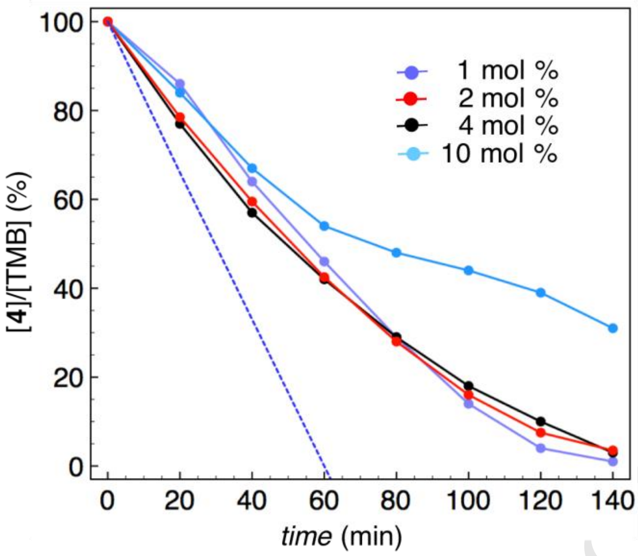

Figure 2. Cyclopropanation of alkene **4** in $CDCl_3$ in the presence of Fe(TPP)Cl with different catalytic loads. Addition of diazomethane precursor **6** into KOH/H_2O solution was carried out at a rate of 1 eq./h. The dashed line corresponds to the theoretical maximum reaction rate associated with conversion of **4** into cyclopropane derivative **5**, assuming instantaneous transformation of **4** into diazomethane and subsequent (2+1) cycloaddition on **4**.

The slow addition of diazomethane precursor **6** may raise questions about the promptness of decomposition of **6** or eventual accumulation of generated diazomethane in the reaction mixture. For this reason, we carried out an experiment to explore what the consequence of sudden cease of addition of **6** would be. Thus, we started the addition rate in the presence of substrate **4** and catalyst **3a** (2 mol %), with an addition rate of 1 eq. of **6** per hour. After 60 min. of reaction time, we stopped this addition (Figure 3). We observed that this interruption induces complete abortion of the reaction progress. This indicates that neither diazomethane nor its precursor **6** was accumulated in the reaction system, despite the less-than-optimal progress of the reaction (*vide supra*).

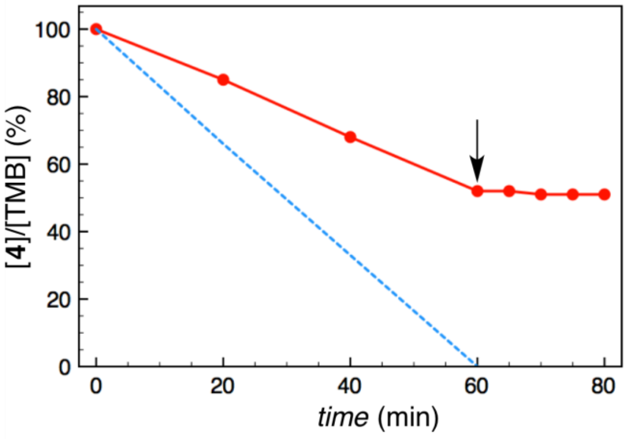

Figure 3. Cyclopropanation of alkene **4** in $CDCl_3$ in the presence of catalyst **3a** (2 % mol), with addition of diazomethane precursor **6** in KOH/H_2O at a rate of 1eq./h. The arrow indicates interruption of addition of **6**. The meaning of the dashed line is that indicated in Figure 2 caption.

Considering the results of the latter experiment (Figure 3), which show that only ca 0.5 equivalents of generated diazomethane were being consumed in the formation of cyclopropane derivative, it can be assumed that at least some part of the remaining 0.5 equivalents was constantly leaking away together with generated nitrogen. This escaping diazomethane was possibly passing directly to the gas phase instead of participating in the cyclopropanation in chloroform.

Experiments testing the performance of metalloporphyrin dendrimers **3b-f** (**G'$_0$-G'$_4$**) on the cyclopropanation reaction of alkene **4** using 2 mol % of catalyst were carried out under same conditions as described previously. Surprisingly, our results showed that the reaction progress was almost unvaried when Fe(TPP)Cl was replaced by simple metalloporphyrins **3a** and **3b** (**G'$_0$**) and also by analogous dendrimers up to the second generation (**3c**, **3d**). However, the reaction rate decreased considerably with the transition to third- (**3e**) and fourth- (**3f**) generation dendrimeric catalysts (Figure 4). The kinetic plots of catalysts **3e** and **3f** showed sigmoidal character, with a relative latency at the beginning of the reaction, during which the progress of the reaction was very slow. This period corresponded to 40 minutes for third-generation dendrimer **3e** and to 2 hours for fourth-generation dendrimer **3f**. Surprisingly, after these induction times the reaction progresses accelerated to rates similar to those found for lower-generation catalysts (Figure 4). In order to ensure that the catalytic activity of these dendrimers rely on the presence of the iron atom, additional blank test with non metallated dendrimers **2b-f** were carried out. As expected, no product formation was observed after 180 min under the described reaction conditions.

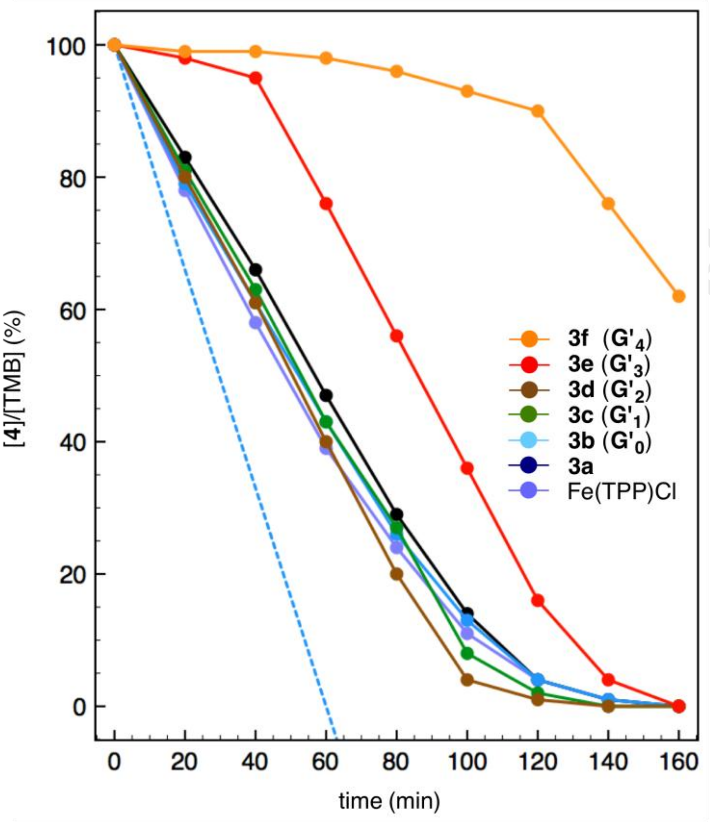

Figure 4. Kinetic profiles corresponding to the conversion of alkene **4** into cyclopropane derivative **5** in the presence of catalysts Fe(TPP)Cl, **3a**, and **3b-f** (**G'$_0$-G'$_4$**). The reaction conditions are those reported in Figure 2 caption.

These results are compatible with a zero-order kinetic behaviour for substrate **4** under the slow injection conditions when small size catalysts are used. Thus, for first and second generation dendrimers **3c** and **3d** the kinetic profiles fit to zero-order kinetics for conversions up to 90 % (the r^2 value was 0.998 in both cases, see Figure 5) according to the following equation:

$$100 - [4] = k_{obs} t \qquad (1)$$

The values obtained for k_{obs} are 0.93 min^{-1} for **3c** (**G'$_1$**) and 0.98 min^{-1} for **3d** (**G'$_2$**), thus confirming the very similar catalytic ability of small dendrimers.

In the case of third and fourth generation dendrimers **3e** and **3f** the respective kinetic profiles were satisfactorily fitted[23] to a standard sigmoidal function of type $S(x)=1/(1+e^{-x})$ in the following form:

$$100 - [4] = \frac{100}{1+exp\left[-\alpha\left(t-\tau\right)\right]} \tag{2}$$

The values obtained for the adjustable exponential parameter α decay on going from third to fourth generation catalysts. Thus, for third generation dendrimer **3e** it was found that α=0.051 min^{-1} and for its fourth generation congener **3f** the corresponding value is α=0.038 min^{-1}. The optimized induction time parameters τ were found to be quite different since for **3e** τ=87 min and in the case of **3f** τ=172 min. As a consequence, when catalyst **3e** is considered an almost linear zero order behaviour is reached for conversions between 20 % (t=60 min) and 80 % (t=120 min), with an apparent slope of 1.00 min^{-1}, a value very close to those found for **3c** and **3d**. In the case of fourth generation catalyst **3f**, the much larger induction time and the lower exponential factor result in a significantly lower catalytic ability.

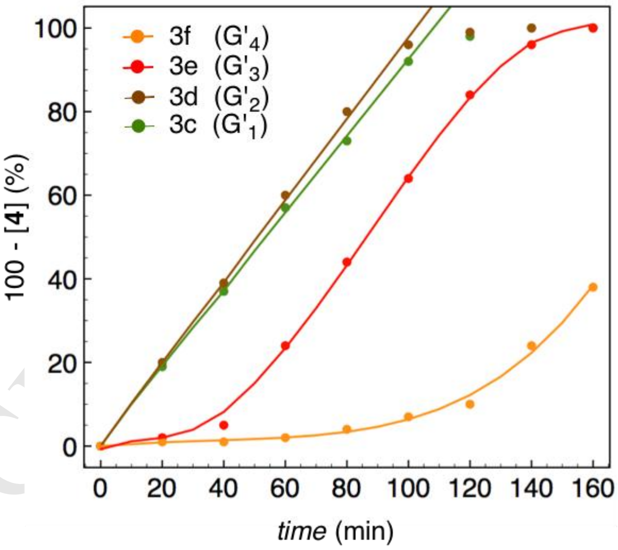

Figure 5. Conversion profiles for catalytic dendrimers **3c-f**. Points correspond to experimental data and lines were obtained by means of eqs. (1) (**3c,d**) and (2) (**3e,f**).

In general, sigmoidal behaviour of kinetic plots can be due to two possible phenomena: autocatalysis[24] and cooperative effects.[25] In the former case, the sigmoidal kinetic profile stems from the acceleration[26] or inhibition[27] generated by the reaction product or by one reactant.[28] In our case, lower catalysts do not show this sigmoidal profile and the reaction product, namely cyclopropane derivative **5** is inert as far as the rate of the (2+1) process is concerned. Therefore, we reasoned that cooperative effects involving dendrimers **3d,f** are most likely due to aggregation processes. It is noteworthy that aggregation[29] and self-assembling[30] phenomena have been observed in dendrimers containing related cores such as phthalocyanines[31], BINOL-Zn complexes,[32] and polyether dendrons.[12,33] In addition, it has been reported that the tendency to aggregation increases with the generation number of the dendrimer.[34]

We investigated the structural properties of metal-free dendrimers **2c-f** using molecular mechanics simulations[35] (see the Experimental Section) in order to get a better understanding of the experimentally observed catalytic effects. We optimized the starting geometries and sampled the different conformations by Molecular Dynamics (MD) simulations. Figure 6 shows the shape of the most stable conformations at 298 K (within 4 kJ/mol) of dendrimers **2c** (**G_1**) and **2d** (**G_2**) in chloroform solution. The geometries thus obtained show that small reactants such as diazomethane and alkene **5** can reach the active site at the core of these dendrimers. This is due to one important feature of these dendrimers, namely the relatively long distance of ca. 16 Å between two collinear branching points at the periphery of the 5,10,15,20-tetraphenylporphyrin core.

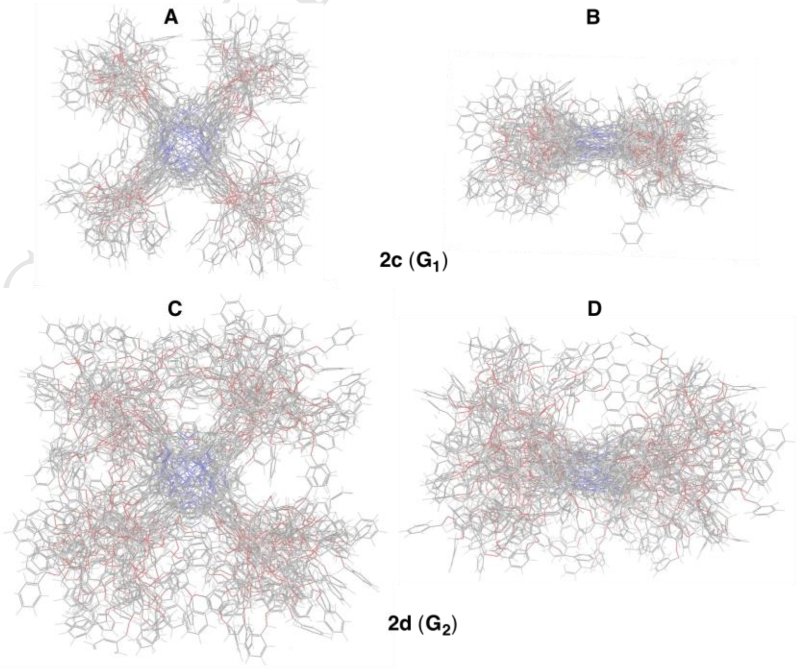

Figure 6. Axial (A and C) and side (B and D) views of the most stable conformations (within 4 kJ/mol) of dendrimers **2c** (**G_1**, A and B) and **2d** (**G_2**, C and D) in chloroform solution. In all cases, porphyrin cores are highlighted in blue.

In order to quantify the shape of dendrimers **2c-f** (**G_1-G_4**), we took the sphere and the cylinder as two extreme models. To do this, we first computed the radius of gyration[36] of each dendrimer of mass M and *n*-atoms of mass m_i as

$$R_g = \left[\frac{1}{M}\sum_{i=1}^{n} m_i\left(\vec{r}_i - \vec{g}\right)\left(\vec{r}_i - \vec{g}\right)\right]^{1/2} \qquad (3)$$

where the position vector of the center of masses is given by

$$\vec{g} = \frac{1}{M}\sum_{i=1}^{n} m_i \vec{r}_i \qquad (4)$$

The square of R_g can be expressed as the trace of the gyration tensor *S* in the form

$$R_g^2 = tr\left(S\right) = tr\begin{pmatrix} L_1^2 & 0 & 0 \\ 0 & L_2^2 & 0 \\ 0 & 0 & L_3^2 \end{pmatrix} \qquad (5)$$

where the three components of the diagonalized tensor *S* are assigned as $L_1^2 > L_2^2 > L_3^2$. With these data, the asphericity[37] a_s of the dendrimer being considered is defined as

$$a_s = L_1^2 - \frac{1}{2}\left(L_2^2 + L_3^2\right) \qquad (6)$$

For a perfect sphere, $L_1^2 = L_2^2 = L_3^2$ holds and hence a_s=0. Therefore, a_s quantifies the departure of the dendrimer from a perfect sphere. Similarly, acyclindricity[34] a_c can be defined as

$$a_c = L_2^2 - L_3^2 \qquad (7)$$

Again, for a perfect cylinder a_c=0 since $L_2^2 = L_3^2$. Low values of a_c permit to identify a shape close to that expected for a cylindric molecular structure. The average values of R_g, a_s and a_c obtained along the MD simulations for **2c**-**f** are reported in Table 1. Asphericity and the evolution of the two latter magnitudes is gathered in Figure 7.

Table 1. Average values[a] of radii of gyration ($\langle R_g \rangle$, in Å), components of the diagonalised tensor S ($\langle L_i \rangle$, in Å), asphericities ($\langle a_s \rangle$, in Å^2) and acylindricities ($\langle a_c \rangle$, in Å^2) of dendrimers **2c-f** (**G$_1$-G$_4$**).

2c-f	$\langle R_g \rangle$	$\langle L_1 \rangle$	$\langle L_2 \rangle$	$\langle L_3 \rangle$	$\langle a_s \rangle$	$\langle a_c \rangle$
G$_1$	9.9 ± 1.1	70.1 ± 1.7	22.7 ± 8.4	7.1 ±1.7	55.1 ± 4.1	15.8 ± 2.4
G$_2$	10.9 ± 0.6	77.0 ± 8.1	32.8 ± 6.8	10.9 ±1.8	54.2 ± 5.5	21.9 ± 5.8
G$_3$	12.7 ± 0.4	77.9 ± 6.5	50.2 ± 5.4	33.7 ± 2.0	35.9 ± 4.9	16.4 ± 6.2
G$_4$	17.0 ± 3.6	197.1 ± 3.7	55.9 ± 2.2	36.3 ±1.5	150.9 ± 4.0	19.5 ±3.3

[a] Average values obtained from MD simulations after 1ns of production time (See Figure 7).

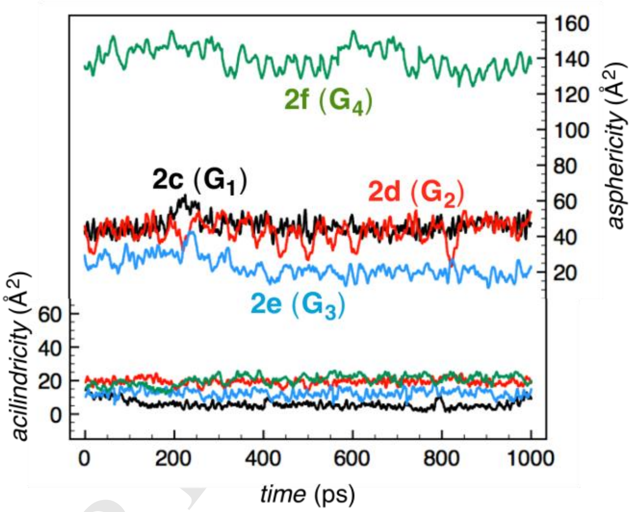

Figure 7. Asphericities and acylindricities of dendrimers **2c-f** along the MD simulations.

Our results indicate that, in effect, the acylindricities for the different generations of dendrimers are quite similar, in agreement with the C$_4$ symmetry axis imposed by the porphyrin moiety. In addition, the asphericities of dendrimers **2c-e** (**G$_1$-G$_3$**) are quite similar and low. These results are compatible with the similar behaviour observed for **3c-e** with respect to **3b** (**G'$_0$**), **3a** and Fe(TPP)Cl. However, the similarities in acylindricity do not provide any clear explanation for the sigmoidal kinetic behaviour of **3e,f** (**G'$_3$**, **G'$_4$**). Since we hypothesized that cooperative effects leading to the formation of aggregates should cause this behaviour, we analysed the aggregation ability of dendrimers **2c** (**G$_1$**) and **2f** (**G$_4$**) by MD simulations in chloroform. At least three interaction models between cylinder-like dendrimers can be envisaged, as it is shown in Figure 8. In the side and axial approaches, both dendrimers interact along parallel or collinear orientations of the two porphyrin systems, as shown in Figure 8, whereas in the case of the perpendicular approach both porphyrin moieties interact along a T-shaped pattern. We tested the three interaction models for $\mathbf{G_1}$ and $\mathbf{G_4}$. The results are gathered in Figure 9.

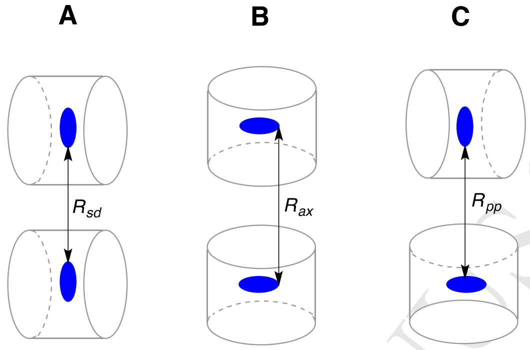

Figure 8. Possible side (A), axial (B) and perpendicular (C) approaches for two units of cylinder-like dendrimers **2e,f** ($\mathbf{G_3}$-$\mathbf{G_4}$). R_{sd}, R_{ax} and R_{pp} denote the minimal distances between the two porphyrin rings.

Our MD simulations show that, after 50 ps of production time, the interacting units of **2c** ($\mathbf{G_1}$) show a very low number of contacts between the two dendrimers even in the case of the axial pattern (Figure 9). Actually, none of the three interaction patterns of $\mathbf{G_1}$ resulted to be dynamically stable, a result compatible with the presence of monomeric catalytic dendrimers **3c** and hence a normal kinetic behaviour in the cyclopropanation reaction. In contrast, fourth generation dendrimer **2f** showed a much slower motion after 50 ps of MD simulation, with dimeric structures of similar energies. Among them, axial and perpendicular interactions were persistent, the former offering more contact surface and shorter distances between the porphyrin moieties (Figure 9). These results are compatible with persistent dimeric or, in general, oligomeric, structures of **2f** ($\mathbf{G_4}$) and therefore for their Fe-containing catalysts **3f** ($\mathbf{G'_4}$).

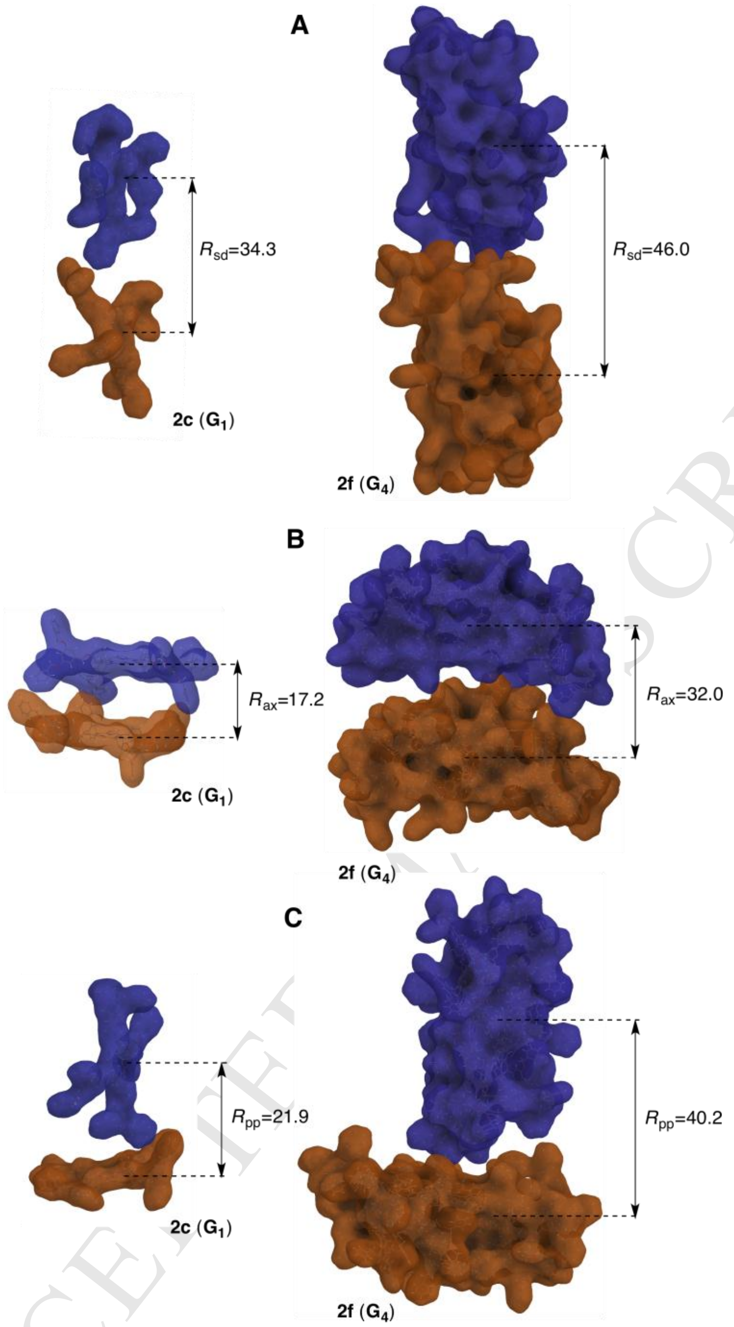

Figure 9. Side (A), axial (B), and perpendicular (C) interaction models for dendrimers **2c** (**G$_1$**) and **2f** (**G$_4$**), after 50 ps of MD simulations in chloroform. Minimal porphyrin-porphyrin distances (See Figure 7) are given in Å. Solvent accessible surfaces (SAS) are shown for the different dendritic units, with a probe radius of 1.4 Å.

We confirmed the distinct aggregation patterns of **2c** and **2f** by performing further MD simulations under periodic boundary conditions (PBC) and with explicit treatment of the solvent. Thus, in the case of **2c** 3,139 molecules of chloroform were included, whereas MD-PBC simulations with **2f** were carried out with a box of similar size including 1,699 molecules of chloroform. The resulting ensembles were stabilized at 298 K and the respective calculations were run at constant temperature and volume for 2 ns.

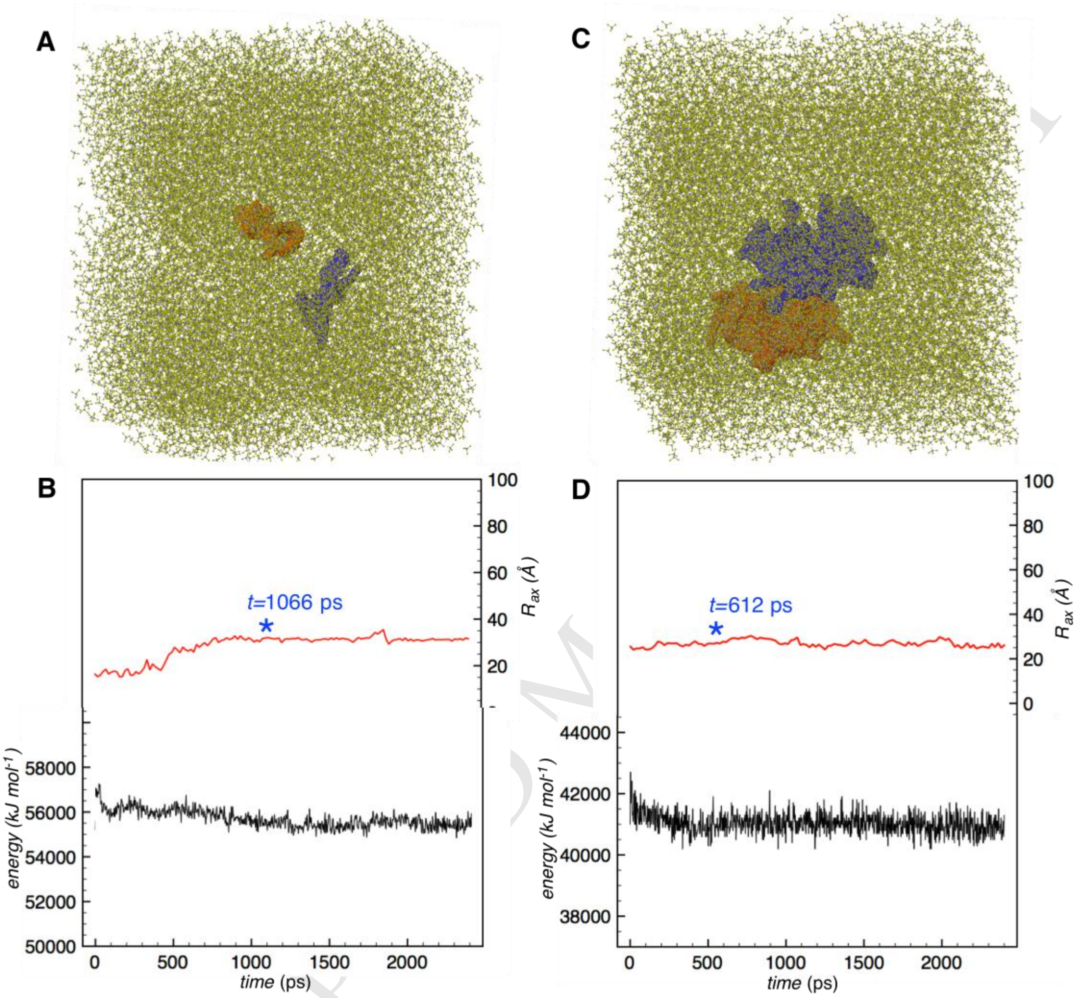

Figure 10. MD-PBC simulations with axial dimeric structures of first and fourth generation dendrimers **2c** (A,B) and **2f** (C,D) in chloroform at 298 K. The solvent accessible surfaces (probe radius: 1.4 Å) for dimers of **2c** (A) and **2f** (C) are indicated. Snapshots gathered in (A) and (C) correspond to the production times indicated in (B) and (D), respectively. The energies and the R_{ax} values along production times for axial dimers corresponding to **2c** (B) and **2f** (D) are also shown.

Our results indicate that the axial dimer of **2c** is not stable: after 612 ps both monomeric structures move independently as in can be observed in Figure 10A,B to reach an average R_{ax} distance of ca. 32 Å. This result confirms that the catalytic behaviour of **3c** (and those associated with low size analogues) can be understood in terms of monomeric intermediates along the catalytic cycle. In contrast, axial dimer of **2f** was stable along the production time, with an average R_{ax} value of ca. 27 Å that permits multiple van der Waals contacts between both dendrimeric units. Therefore, explicit treatment of the solvent compresses the dimeric structures and shows that these aggregates are not fleeting species. By extension, we concluded that fourth generation dendrimers could exist as dimers and higher order aggregates combining the three kinds of approaches shown in Figures 8 and 9. On the basis of its similar sigmoidal behaviour, third generation dendrimers will exhibit a similar tendency to form aggregates.

To verify experimentally the different behaviour of metal free non-paramagnetic dendrimers **2c** and **2f**, we carried out different Diffusion-Ordered NMR Spectroscopy[38] (DOSY) experiments with these compounds at several concentrations in $CDCl_3$. We performed ^{1}H-DOSY experiments because of the high sensitivity of this technique, which permitted measurements at relatively low concentrations, especially in the case of fourth generation dendrimer **2f**. Figure 11 shows the 2D spectra for both compounds, in which we have represented in the x-axis the part of the ^{1}H spectra corresponding to the benzylic signals associated with the Ar-CH_2-O moieties of both dendrimers. We observed that the relative diffusion rates for these signals were similar and easier to monitor at low concentrations (see the y-axes of Figure 11). The respective diffusion coefficients are gathered in Table 2.

Table 2. Diffusion parameters of dendrimers **2c**,**f** (**G_1**,**G_4**).

Dendrimer	Conc. (mg/mL)	D (m^2/s)[a]	r_H (Å)[b]
2c (G_1)	11	5.44×10^{-10}	11.1
2c (G_1)	54	5.44×10^{-10}	11.1
2f (G_4)	7	4.76×10^{-10}	12.7
2f (G_4)	36	3.34×10^{-10}	18.1
2f (G_4)	40	2.51×10^{-10}	24.1

[a]Diffusion parameters D obtained by 2D ^{1}H-DOSY experiments. [b]Diffusion radii estimated by means of the Stokes-Einstein equation with C=4.

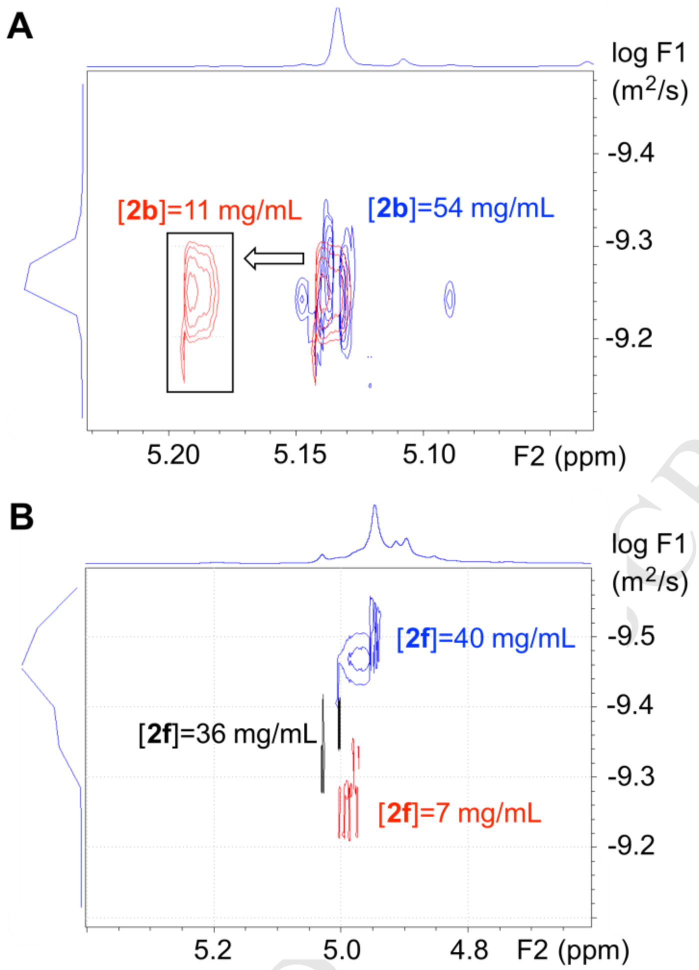

Figure 11. 2D ^{1}H-NMR data for dendrimers **2b** (A) and **2f** (B) in $CDCl_3$ at different concentrations. The inset in (A) corresponds to signals for **2b** at 11 mg/mL.

In the case of **2c** (**G$_1$**), we measured similar diffusion coefficients at relatively high concentrations of 11 mg/mL and 54 mg/mL. These values correspond to identical diffusion radii r_H estimated by means of the Stokes-Einstein[39] theory:

$$D = \frac{k_B T}{C p h r_H} \tag{8}$$

According to eq. (8) the diffusion coefficient D varies inversely with the size of a hypotethical sphere of radius r_H. k_B is the Boltzmann's constant, η is the viscosity of the surrounding fluid (in our case chloroform, for which η=5.42 x 10^{-4} Pa/s at 298 K) and C is a constant that depends on the boundary conditions at the particle-solvent interface, and varies from C=6 to C=4 for spherical particles. From our NMR data we obtained for **2c** (**G$_1$**) the r_H value reported in Table 2 for C=4, which corresponds to approximate spheres associated with monomeric species moving under slip boundary conditions.[40] This result is in line with the radius of gyration of ca. 10 Å computed for monomeric **2c** (see Table 1). Therefore, on the basis of the ^{1}H-DOSY data, we concluded that, in agreement with our kinetic and MD data, first generation dendrimer **2b** (**G$_1$**) does not aggregate significantly, at least up to the highest concentration studied.

The situation changed when the behaviour of dendrimer **2f** (**G$_4$**) was analysed at different concentrations (Table 2). In this case, we obtained different *D* values at different concentrations. Interestingly, the diffusion coefficients *D* obtained from the ^{1}H-DOSY experiments decreased, as the samples were more concentrated. At our lowest concentration of 7 mg/mL the r_H value was also the lowest one, slightly smaller than -but comparable to- the average radius of gyration of ca. 17 Å. At our highest concentration of 40 mg/mL (we could not obtain accurate NMR spectra at higher concentrations because of solubility issues), the r_H value is of the same magnitude that (but slightly higher than) our computed radius for the dimer of **2f** (**G$_4$**), which was calculated to be of ca. 21 Å. On the basis of these results, we concluded that at the concentrations studied, higher generation dendrimer **2f** (**G$_4$**) forms dimers and, most likely, higher aggregates.

From our MD computational data and our DOSY NMR results, we interpret our kinetic experimental results in terms of the tendency of third and fourth generation dendrimers to form aggregates that result in a cooperative effect. First, higher generation dendrimeric aggregates capture the incoming diazomethane. The resulting intermediate carbene complexes can be buried inside the oligomeric structures and only after saturation of the aggregates the (2+1) cycloaddition reaction starts to proceed efficiently. In addition, generation of more accessible Fe-carbene complexes on the surface of the aggregates and/or perturbation of the A-B equilibria (Scheme 3) and the corresponding preferred spin states cannot be ruled out. The final outcome is that these Fe-porphyrin aggregates show cooperative effects and sigmoidal kinetic plots similar to those observed in protein analogues such as cytochromes[41] and haemoglobin.[42]

Conclusions

In this work we report the preparation and assessment of the catalytic properties of different generations of dendrimers based on Fe(porphyrin) catalytic cores. These formally D_{4h}-symmetric dendrimers incorporate polyether Fréchet dendritic arms around the 5,10,15,20-tetrakis(4-hydroxyphenyl)porphyrin moiety. The reaction studied is the (2+1) cyclopropanation of a model alkene in the presence of diazomethane, safely and efficiently generated using the method reported by Morandi and Carreira. In contrast with the kinetic behaviour observed for other dendrimers with only one catalytic centre at the core, the reaction proceeds with rates comparable to those observed for the Fe(TPP)Cl catalyst. Thus, dendrimers from zeroth to second generation exhibit a normal linear pseudo zero order behaviour, with similar reaction rates. Structural parameters computed for these dendrimers are compatible with this result. In contrast, third and fourth generation dendrimers show sigmoidal kinetic plots, with increasing induction times on going from the third to the fourth generation. Beyond that point, the cyclopropanation reactions proceed and in the case of third generation catalyst the observed rate was comparable to those observed for lower generation catalysts. This distinct behaviour has been attributed to cooperative effects, generated via aggregation of dendritic units, a process that is only kinetically relevant for higher generations of dendrimers possessing large surfaces available for axial, side or perpendicular dendrimer-dendrimer contacts. This interpretation is compatible with molecular dynamics simulations. Finally, our results suggest that these macromolecules are efficient catalysts for the cyclopropanation of other alkenes under safe conditions, thus exploiting the advantages of dendrimers as catalysts.

Experimental section

General experimental methods: Reagents and solvents were purchased from commercial suppliers and used without further purification. Reagents used were of ACS reagent grade. Flash chromatography separations were carried out using silica gel 60 (0.040 – 0.063 mm) if not stated otherwise. NMR spectra were recorded at Varian Gemini 300 HC spectrometer or at Bruker Avance 500 spectrometer. HRMS (ESI+) spectra were recorded using LTQ Orbitrap Velos (Thermo Scientific) instrument. UV-Vis spectra were recorded at Tecan Infinite 200 Pro spectrophotometer in range of 250-700 nm. Analytical TLC was performed on Merck TLC Silica gel 60 F_{254} plates using visualization by UV light at 254 nm and 365 nm. MS MALDI-TOF spectra were recorded on UltrafleXtreme MALDI-TOF/TOF mass spectrometer (Bruker Daltonics, Germany), using a 0.3 M solution of indoleacrylic acid in THF as matrix.

Water-soluble diazomethane precursor **6** was prepared following the procedure reported by Morandi and Carreira[13]. 3-(*N*-Methyl-*N*-nitrososulfamoyl)benzoic acid (90 mg, 0.33 mmol, 90% purity) was suspended in water (2.7 ml) and $NaHCO_3$ (35 mg, 0.42 mmol) was added portionwise under stirring. The mixture was stirred for 1 hour, filtered and the resulting solution of **6** was used immediately in kinetic experiment. Precursor 3-(*N*-methyl-*N*-nitrososulfamoyl)benzoic acid was purified by dissolution in a minimum quantity of dichloromethane, filtration and precipitation by pentane from the filtrate. The precipitate was dried under high vacuum. Its ^1H NMR analysis in methanol permitted to verify the ratio of nitrosation, comparing integrals of methyl group signals of this compound and its precursor 3-(*N*-methylsulfamoyl)benzoic acid. Using this method, 90% pure 3-(*N*-methyl-*N*-nitrososulfamoyl)benzoic acid was prepared, with remaining 10% of 3-(*N*-methylsulfamoyl)benzoic acid as impurity. Purified 3-(*N*-methyl-*N*-nitrososulfamoyl)benzoic acid was stored in a freezer under argon and was used in next few days in order to ensure unvaried purity of **6** in catalytic experiments. Otherwise, it was observed that 3-(*N*-methyl-*N*-nitrososulfamoyl)benzoic acid slowly decomposes by denitrosation back to 3-(*N*-methylsulfamoyl)benzoic acid if let at room temperature.

Procedures for the synthesis of metalloporphyrin catalysts: Polyaromatic Fréchet dendrons, of generation number one to four, Br-$D_{1\text{-}4}$, were prepared following the reported procedure. Their spectral properties were in accordance with those reported in the literature.[19] 5,10,15,20-Tetraphenylporphyrin iron(III) chloride (Fe(TPP)Cl) was prepared from commercial tetraphenylporphyrin as described previously.[15]

5,10,15,20-tetrakis(4-methoxyphenyl)porphyrin (2a): Commercial 5,10,15,20-tetrakis(4-hydroxyphenyl)porphyrin **1** (100 mg, 0.147 mmol) was dissolved in DMF (3 ml). To this solution K_2CO_3 (200 mg, 1.45 mmol), 18-crown-6 (5 mg, 0.019 mmol) and iodomethane (1.14 g, 8.02 mmol, 0.5 ml) were added. Reaction mixture was protected from light and stirred for 20 hours at 70 °C under argon. Then, the solvent was removed under reduced pressure. The resulting mixture was dissolved in CH_2Cl_2, filtered and deposed on a column of alumina (neutral, Brockman II). During the column separation 4 % of THF in CH_2Cl_2 was used as mobile phase. After the precipitation by hexane from CH_2Cl_2, the title product was obtained as purple solid in 45 % yield (64 mg, 0.066 mmol). Spectral properties of this compound were in accordance with those reported in the literature[43], in which another procedure for the preparation of title compound is reported.

5,10,15,20-tetrakis(4-benzyloxyphenyl)porphyrin (2b): 5,10,15,20-tetrakis(4-hydroxyphenyl)porphyrin **1** (100 mg, 0.147 mmol) was dissolved in DMF (3 ml). To the solution K_2CO_3 (200 mg, 1.45 mmol), 18-crown-6 (5 mg, 0.019 mmol) and benzyl bromide (0.72 g, 4.21 mmol) were added. Reaction mixture was protected from light and stirred for 20 hours at 70 °C under argon. Then, the solvent was removed under reduced pressure. The resulting mixture was dissolved in CH_2Cl_2, filtered, deposed on a column of alumina (neutral, Brockman II) and purified by column separation using 4 % (v/v) of Et_2O in CH_2Cl_2 as mobile phase. After evaporation and precipitation with an appropriate hexane/CH_2Cl_2 mixture, the title product was obtained as a purple solid in 40 % yield (58 mg, 0.056 mmol). Spectral properties of this compound were in accordance with those reported in the literature,[44] in which another procedure for the preparation of title compound is reported.

Porphyrin dendrimers 2c-e: these compounds were prepared from 5,10,15,20-tetrakis(4-hydroxyphenyl)porphyrin **1** and bromides Br-D_{1-3} following the method reported by Matos, Fréchet et al. and their spectral properties were in accordance with the literature.[45]

Porphyrin dendrimer 2f: 5,10,15,20-Tetrakis(4-hydroxyphenyl)porphyrin **1** (6.7 mg, 0.010 mmol) was dissolved in mixture of DMF (1 ml) and toluene (1 ml). To this solution K_2CO_3 (30 mg, 0.217 mmol), 18-crown-6 (5 mg, 0.019 mmol) and Br-D_4 (200 mg, 0.060 mmol) were added. The resulting reaction mixture was protected from light and stirred for 20 hours at 70 °C under argon. Then, it was diluted by CH_2Cl_2 and extracted twice with brine. The organic phase was dried by $MgSO_4$, filtered and evaporated under reduced pressure. The residue was purified by flash chromatography on silica gel (toluene/CH_2Cl_2) and by precipitation with an appropriate mixture of hexanes/CH_2Cl_2 to afford the title product as purple glass in 36 % yield (50 mg, 0.0036 mmol). ^{1}H NMR (500 MHz, $CDCl_3$): δ = -2.75 (s, 2H, N*H*), 4.82-4.93 (m, 224 H, C*H*$_2$O), 4.97 (s, 16 H, C*H*$_2$O), 5.13 (s, 8 H, C*H*$_2$O), 6.41-6.71 (m, 172 H, Ar-*H*), 6.83 (br s, 8 H, Ar-*H*), 7.17-7.39 (m, 328 H, phenyl H, phenylene H-3,5), 8.04 (d, 8 H, phenylene H-2,6, J = 7,6 Hz), 8.82 (s, 8 H, porphyrin H). ^{13}C NMR (126 MHz, $CDCl_3$): δ = 69.85, 69.95, 70.03 (CH_2O), 101.48, 106.29, 106.32, 106.38, 127.47, 127.49, 127.53, 127.91, 127.97, 128.47, 128.49, 128.55, 136.68, 139.15, 159.98, 160.05 (Ar, porphyrin, phenylene). UV-Vis (THF) λ_{max}: 425 nm, 518 nm, 557nm, 598 nm, 650 nm. MS (MALDI-TOF) *m/z* calculated 13774.9 $[M+H]^+$, found 13774.3.

General procedure for the synthesis of metalloporphyrins and dendrimers 3: The corresponding free-base porphyrin **2** and $FeCl_2$ were dissolved in dry THF and the reaction mixture thus obtained was refluxed under argon and under protection from light for 20 hours. After cooling of the solution to room temperature, the mixture was exposed to open air under further stirring for 20 minutes. The solvent was evaporated and the obtained residue was purified by flash chromatography on silica gel, using CH_2Cl_2/MeOH as mobile phase, in order to remove unreacted $FeCl_2$. Observation of decay of Soret peak in measured UV-Vis spectra permitted to monitor completion of iron insertion.[20a]

Metalloporphyrin 3a: The title compound was prepared as an orange-brown solid in 90 % yield (92 mg, 0.815 mmol) from $FeCl_2$ (130 mg, 1.03 mmol), free-base porphyrin **2a** (100 mg, 0.096 mmol) and THF (30 ml). UV-Vis (THF) λ_{max}: 414, 578, 620. HRMS (ESI+): *m/z* calculated 788.20805 $[M+H]^+$, found 788.20752. Preparation of this compound was reported previously[46] but spectral properties are unavailable in the literature.

Metalloporphyrin 3b (G_0): The title compound was prepared as an orange-brown solid in 85 % yield (160 mg, 0.0.085 mmol) from $FeCl_2$ (120 mg, 0.947 mmol), free-base porphyrin **2b** (40 mg, 0.054 mmol) and THF (12 ml). UV-Vis (THF) λ_{max}: 412, 578, 620. HRMS (ESI+): *m/z* calculated 1092.33325 $[M+H]^+$, found 1092.33331. Preparation of this compound was reported previously[42] but spectral properties are unavailable in the literature.

Metalloporphyrin 3c (G_1): The title compound was prepared as an orange-brown solid in 76 % yield (128 mg, 0.0647 mmol) from $FeCl_2$ (110 mg, 0.868 mmol), free-base porphyrin dendrimer **2c** (160 mg, 0.0.085 mmol) and THF (25 ml). UV-Vis (THF) λ_{max}: 412, 576, 616. HRMS (ESI+): *m/z* calculated 1941.67152 $[M+H]^+$, found 1941.67040.

Metalloporphyrin 3d (G_2): The title compound was prepared as an orange-brown solid in 90 % yield (125 mg, 0.0340 mmol) from $FeCl_2$ (100 mg, 0.785 mmol), free-base porphyrin dendrimer **2d** (135 mg, 0.0375. mmol) and THF (21 ml). UV-Vis (THF) λ_{max}: 423, 582, 616. MS (MALDI-TOF): *m/z* calculated 3639.9 $[M]^+$, found 3640.2, loss of C_7H_6 (calc. *m/z* 3549.9, found 3549.8).

Metalloporphyrin 3e (G_3): The title compound was prepared as an orange-brown solid in 96 % yield (35 mg, 0.0025 mmol) from $FeCl_2$ (100 mg, 0.785 mmol), free-base porphyrin dendrimer **2e** (115 mg, 0.0165 mmol) and THF (25 ml). UV-Vis (THF) λ_{max}: 422, 506 (very weak), 576 (very weak). MS (MALDI-TOF): *m/z* calculated 7035.9 $[M]^+$, found 7035.4; loss of C_7H_6 (calc. *m/z* 6945.8, found 6945.9).

Metalloporphyrin 3f (G_4): The title compound was prepared as an orange-brown solid in 75 % yield (112 mg, 0.0158 mmol) from $FeCl_2$ (25 mg, 0.197 mmol), free-base porphyrin dendrimer **2e** (45 mg, 0.0033 mmol) and THF (5 ml). UV-Vis (THF) λ_{max}: 424, 508 (very weak), 582 (very weak). MS (MALDI-TOF): *m/z* calculated 13827.7 $[M]^+$, found 13853.1.

General procedure for the kinetic experiments with catalysts 3a-d: A solution of 1-chloro-4-(prop-1-en-2-yl)benzene **4** (16.7 mg, 0.110 mmol, 0.016 ml), 1,2,3-trimethoxybenzene (internal standard, 10 mg, 0.059 mmol) and the corresponding metalloporphyrin catalyst **3a-d** (2 mol%, 0.0022 mmol) in $CDCl_3$ (0.4 ml) was added to an aqueous solution of KOH (6 M, 1 ml) in a 5 ml flask sealed with a septum. The resulting biphasic mixture was vigorously stirred for 5 minutes. Then, keeping the magnetic stirring, slow addition of freshly prepared aqueous solution of diazomethane precursor **6** (0.122 M, 2.7 ml) was started using an automatic syringe pump, keeping the addition rate at 0.9 ml/hour, which corresponds to 1 equivalent of **6** per hour. At the start of the addition, an open 1 ml plastic syringe without plunger, previously filled with a KOH solution (6 M, 0.3 ml), was introduced into the flask via needle to lead off excess of gas phase during the addition process. Aliquots of 0.020 ml were withdrawn from the organic phase by means of a microsyringe after a short cease of stirring. The aliquots were withdrawn every 20 minutes after the start of the addition of **6** solution and also shortly before starting the experiment. The aliquots were diluted by $CDCl_3$ to stop the reaction and analysed by ^{1}H NMR. The reaction progress was monitored by calculation of substrate concentration decrease from the NMR data of the crude reaction mixture. Integrals of the ^{1}H-NMR signal of the substrate methyl group (δ, ppm: 2.12) in each sample were compared with the integral of internal standard methyl groups (δ, ppm: 3.87, 3.86), using the aliquot taken before starting the addition of **6** as reference.

Blank experiments were performed under identical conditions but in the absence of catalysts **3**. No reaction progress was observed during the time of 3 hours.

Experiment with interruption of the addition of diazomethane precursor **6** was carried out by following the general procedure using metalloporphyrin **3a** as catalyst, but the addition of **6** solution was stopped after 60 minutes. Since that moment, aliquots were withdrawn every 5 minutes during the next 20 minutes. No significant reaction progress was observed after interruption of the addition of **6**.

Procedure for the kinetic experiments using 3e or 3f as catalysts: Under the conditions reported for the previous general procedure, metallodendrimers **3e** and **3f** formed emulsions when stirred in the biphasic system, which could result in a slower progress of the reaction. To avoid the formation of emulsions, the flask size was changed from 12 x 45 mm to 15 x 55 mm and the size of the magnetic stirrer bar from 5 x 12 mm to 8 x 12 mm. The amount of $CDCl_3$ used was increased to 0.6 ml.

1,2,3-Trimethoxybenzene (internal standard): This compound is commercially available and was used without further purification. ^{1}H NMR (500 MHz, $CDCl_3$): δ = 3.86 (s, 3H, OCH_3), 3.87 (s, 6H, OCH_3), 6.59 (d, 2H, ArH), 7.00 (t, 1H, ArH)**.**

1-Chloro-4-(prop-1-en-2-yl)benzene (4): this compound is commercially available and was used without further purification. ^{1}H NMR (500 MHz, $CDCl_3$): δ = 2.12 (s, 3H, $-CH_3$), 5.09 (s, 1H, $=CH_2$), 5.34 (s, 1H, $=CH_2$), 7.28 (d, 2H, ArH, J = 8.51 Hz), 7.38 (d, 2H, ArH, J = 8.80 Hz).

1-Chloro-4-(1-methylcyclopropyl)benzene (5): this (2+1) cycloadduct was obtained as colourless oil by column chromatography from the different reaction mixtures following the general procedure for kinetic experiments. Spectral properties are in accordance with those reported in the literature.[13] ^{1}H NMR (500 MHz, $CDCl_3$): δ = 0.70-0.75 (m, 2H, CH_2), 0.80-0.84 (m, 2h, CH_2), 1.38 (s, 3H, CH_3), 7.14-7.24 (m, 4H, Ar*H*).

^{1}H-DOSY experiments: The different experiments were carried out on a Bruker 500 AVANCE equipped with a *z*-gradient BBO probe. Each DOSY experiment was recorded using the *lebbpgp2s* sequence. The number of scans was 16. The strength of the gradient was changed from 2 % to 95% using a 50 G cm^{-1} gradient unit. The value of big delta Δ was 200 ms and little delta δ was 800 ms. A delay of 5 ms was used to avoid the formation of eddy currents.

Computational methods: All the computational studies reported in this paper were based upon molecular mechanics[47] (MM) and molecular dynamics (MD).[48] In both, the MM3 method developed by Allinger et al. as implement in the MacroModel[49] package was used. All MD simulations were performed with SHAKE[50] to constrain the C-H bonds. The temperature was set up to 298 K. The system was equilibrated for 1 ns with time steps of 1 fs. This equilibration time is 10 times longer than the expected value for the relaxation time of dendrimers[51] of this size. The production run was started from this point and lasted another nanosecond with time steps of 1 fs. In all cases, we observed that during the production period, the energy and temperature of the whole system were equilibrated. During the production run, the coordinates were saved each picosecond, which implies a total of 1000 structures. These structures were used to calculate the averages of the properties specified below. To calculate these properties, programs based on the DYNAMO library[52] were written. In the case of MD simulations under periodic boundary conditions (MD-PBC) in chloroform, a specific force field potential optimized for liquid simulations (OPLS_2005)[53] was used as implemented on Desmond package.[54] These simulations were performed using periodic boundary conditions within the canonical NVT ensemble at 298.15 K and a cubic box of 90 Å of side length. The system was equilibrated for 2 ns with time steps of 1 ps.

Acknowledgements

The work carried out by the Czech authors was supported by the Ministry of Education, Youth and Sports of the Czech Republic (Project MSM6046137305) and by the Czech Science Foundation (Projects 304/10/1951 and P503/11/0616). P. V. also thanks the DIPC for a visiting fellowship. Financial support to the Spanish authors was provided by the Ministerio de Economía y Competitividad (MINECO) of Spain and FEDER (project CTQ2013-45415-P), the UPV/EHU (UFI11/22 QOSYC), and the Basque Government (GV/EJ, grant IT-324-07). The authors thank the SGI/IZO-SGIker UPV/EHU and the DIPC for generous allocation of computational and analytical resources.

References

---

[1] (a) Bosman, A. W.; Janssen, H. M.; Meijer, E. W. *Chem. Rev.* **1999**, *99*, 1665-1688. (b) Astruc, D.; Chardac, F. *Chem. Rev.* **2001**, *101*, 2991-3023. (c) Twyman, L. J.; King, A. S. H.; Martin, I. K. Chem. Soc. Rev. **2002**, *31*, 69-82. (d) Kofoed, J.;

Raymond, J.-L. *Curr. Opin. Chem. Biol*. **2005**, *9*, 656-664. (e) Darbre, T.; Reymond, J.-L. *Acc. Chem. Res.* **2006**, *39*, 925-934. (f) Liang, C. J.; Fréchet, M. J. *Prog. Polym. Sci*. **2005**, *30*, 385-402. (g) Astruc, D.; Boisselier, E.; Ornelas, C. *Chem. Rev.* **2010**, *110*, 1857-1959. (h) John, A.; Natchigall, F. M.; Santos, L. S. *Curr. Org. Chem*. **2012**, *16*, 1776-1787. (i) Li, Z.; Li, J. *Curr. Org. Chem*. **2013**, *17*, 1334-1349. (j) Bronstein, L. M. *ChemCatChem* **2015**, *7*, 1058-1060.

[2] (a) Bagul, R. S.; Jayaraman, N. *Inorg. Chim. Acta* **2014**, *409*, 34-52. (b) Caminade, A.-M.; Ouali, A.; Laurent, R.; Majoral, J.-P. *Inorg. Chim. Acta*, **2015**, *431*, 3-20. (c) El Brahmi, N.; El Kazzouli, S.; Mignani, S.; Bousmina, M.; Majoral, J. P. *Tetrahedron* **2013**, *69*, 3103-3133. (d) Wang, D.; Astruc, D. *Coord. Chem. Rev*. **2013**, *257*, 2317-2334. (e) Astruc, D.; Liang, L.; Rapakousiou, A. J. Ruiz, *Acc. Chem. Res.* **2012**, *45*, 630-640. (f) He, Y.-M.; Feng, Y.; Fan, Q.-H. *Acc. Chem. Res.* **2014**, *47*, 2894-2906. (g) Caminade, A.-M.; Servin, P.; Laurent, R.; Majoral, J.-P. *Chem. Soc. Rev*. **2008**, *37*, 56-67. (h) Astruc, D.; Ornelas, C.; Ruiz, J. *Acc. Chem. Res*. **2008**, *41*, 841-856. (i) Andrés, R.; de Jesús, E.; Flores, J. C. *New. J. Chem*. **2007**, *31*, 1161-1191. (j) Méry, D.; Astruc, D. *Coord. Chem. Rev*. **2006**, *250*, 1965-1979. (k) Oosterom, G. E.; Reek, J. N. H.; Kamer, P. C. J.; van Leeuwen, P. W. N. M. *Angew. Chem. Int. Ed.* **2001**, *40*, 1828-1849.

[3] (a) Caminade, A.-M.; Ouali, A.; Keller, M.; Majoral, J.-P. *Chem. Soc. Rev*., 2012, **41**, 4113-4125. (b) Rasmussen, B.; Christensen, J. B. *Org. Biomol. Chem*., 2012, **10**, 4821-4835.

[4] Heuzé, K.; Méry, D.; Gauss, D.; Astruc, D. *Chem. Commun.*, 2003, 2274-2275.

[5] Dijkstra, H. P.; van Klink, G. P. M.; van Koten, G. *Acc. Chem. Res*., 2002, **35**, 798-810.

[6] Helms, B.; Fréchet, J. M. J. *Adv. Synth. Catal.* **2006**, *348*, 1125-1148.

[7] Malkoch, M.; Hallman, K.; Lutsenko, S.; Hult, A.; Malmström, E.; Moberg, C. *J. Org. Chem.* **2002**, *67*, 8197-8202.

[8] Rheiner, P. B.; Seebach, D. *Chem. Eur. J.* **1999**, *5*, 3221-3236.

[9] (a) Mak, C. C.; Chow, H.-F. *Macromolecules* **1997**, *30*, 1228-1230. (b) Andrés, R.; de Jesús, E.; de la Mata, F. J.; Flores, J. C.; Gómez, R. *Eur. J. Inorg. Chem.* **2002**, 2281-2286.

---

[10] Zubia, A.; Cossío, F. P.; Morao, I.; Rieumont, M.; Lopez, X. *J. Am. Chem. Soc*. **2004**, *126*, 5243-5252.

[11] Morao, I.; Cossío, F. P. *Tetrahedron Lett*. **1997**, *38*, 6461-6464.

[12] Vinš, P.; Vermachová, M.; Drašar, P.; del Barrio, M.; Jarne, C.; Cebolla, V. L.; de Cózar, A.; Zangi, R.; Cossío, F. P. *Tetrahedron* **2013**, *69*, 10361-10368.

[13] Morandi, B.; Carreira, E. M. *Science* **2012**, *335*, 1471-1474.

[14] (a) Intrieri, D.; Caselli, A.; Gallo, E. *Eur. J. Inorg. Chem*. **2011**, 5071-5081. (b) Anding, B. J.; Ellern, A.; Woo, L. K. *Organometallics* **2012**, *31*, 3628-3635. (c) Doyle, M. P. *Angew. Chem., Int. Ed*. **2009**, *48*, 850-852. (d) Gross, Z.; Galili, N.; Simkhovich, L. *Tetrahedron Lett*. **1999**, *40*, 1571-1574. (e) Huang, L.; Chen, Y.; Gao, G.-Y.; Zhang, X. P. *J. Org. Chem*. **2003**, *68*, 8179-8184. (f) Morandi, B.; Dolva, A.; Carreira, E. M. *Org. Lett*. **2012**, *14*, 2162-2163. (g) Nicolas, I.; le Maux, P.; Simonneaux, G. *Tetrahedron Lett*. **2008**, *49*, 5793-5795. (h) Wurz, R. P.; Charette, A. B. *Org. Lett*. **2002**, *4*, 4531-4533. (i) Maas, G. *Chem. Soc. Rev*. **2004**, *33*, 183-190.

[15] Sun, Z.-C.; She, Y.-B.; Zhou, Y.; Song, X.-F.; Li, K. *Molecules* **2011**, *16*, 2960-2970.

[16] Schoental, R. *Nature* **1960**, *188*, 420-421.

[17] Li, W.-S.; Aida, T. *Chem. Rev*. **2009**, *109*, 6047-6076.

[18] Grayson, S. M.; Fréchet, J. M. J. *Chem. Rev*. **2001**, *101*, 3819-3867.

[19] Hawker, C. J.; Fréchet, J. M. J. *J. Am. Chem. Soc*. **1990**, *112*, 7638-7647.

[20] (a) Shema-Mizrachi, M.; Pavan, G. M.; Levin, E.; Danani, A.; Lemcoff, N. G. *J. Am. Chem. Soc.* **2011**, *133*, 14359-14367. (b) Che, C.-M.; Huang, J.-S.; Zhang, J.-L. *C. R. Chimie* **2003**, *6*, 1105-1115.

[21] (a) Wolf, J. R.; Hamaker, C.G.; Djukic, J.-P.; Kodadek, T.; Woo, L. K. *J. Am. Chem. Soc.* **1995**, *117*, 9194-9199. (b) Hamaker, C. G.; Mirafzal, G. A.; Woo, L. K. *Organometallics* **2001**, *20*, 5171-5176. (c) Lai, T.-S.; Chan, F.-Y.; So, P.-K.; Ma, D.-L.; Wong, K.-Y.; Che, C.-M. *Dalton Trans.* **2006**, 4845-4851.

[22] (a) Tatsumi, K.; Hoffman, R. *Inorg. Chem.* **1981**, *20*, 3771-3784. (b) Latos-Grażyński, I.; Cheng, R.-J.; La Mar, G. N.; Balch, A. L. *J. Am, Chem. Soc.* **1981**, *103*, 4270-4272. (c) Olmstead, M. M.; Cheng, R.-J.; Balch, A. L. *Inorg. Chem*, **1982**, *21*, 4143-4148. (d) Balch, A. L.; Cheng, R.-J.; La Mar, G. N.; Latos-Grażyński, L. *Inorg. Chem.* **1985**, *24*, 2651-2656. (e) Artaud, I.; Gregoire, N.; Leduc, P.; Mansuy, D. *J. Am. Chem. Soc.* **1990**, *112*, 6899-6905.

---

[23] Wolfram Research, Inc., *Mathematica*, Version 8.0, Champaign, IL, **2010**.

[24] Steinfeld, J. I.; Francisco, J. S.; Hase, W. L. *Chemical Kinetics and Dynamics (2nd Ed.)*, Prentice Hall: New Jersey, **1999**, pp. 151-153.

[25] Bisswanger, H. *Enzyme Kinetics –Principles and Methods (2nd Ed.)*; Wiley-VCH: Weinheim, **2008**; pp. 32-56.

[26] Mathew, S. P.; Klussmann, M.; Iwamura, H.; Wells Jr., D. H.; Armstrong, A.; Blackmond, D. G. *Chem. Commun*. **2006**, 4291-4293.

[27] Phua, P. H.; Mathew, S. P.; White, A. J. P.; de Vries, J. G.; Blackmond, D. G.; Hii, K. K. *Chem. Eur. J*. **2007**, *13*, 4602-4613.

[28] Mower, M. P.; Blackmond, D. G. *J. Am. Chem. Soc*. **2015**, *137*, 2386-2391.

[29] (a) Wang, B.-B.; Zhang, X.; Jia, X.-R.; Li, Z.-C.; Li, Y.; Yang, L.; Wei, Y. *J. Am. Chem. Soc.* **2004**, *126*, 15180-15194. (b) Jasmine, M. J.; Kavitha, M.; Prasad, E. *J. Lumin.* **2009**, *129*, 506-513.

[30] (a) Dong, R.; Zhou, Y.; Zhou, Z. *Acc. Chem. Res*. **2014**, *47*, 2006-2016. (b) Raghupathi, K. R.; Guo, J.; Munkhbat, O.; Rangadurai, P.; Thayumanavan, S. *Acc. Chem. Res*. **2014**, *47*, 2200-2211.

[31] Ng, D. K. P. *C. R. Chim*. **2003**, *6*, 903-910.

[32] Hu, Q.-S.; Pugh, V.; Sabat, M.; Pu, L. *J. Org. Chem*. **1999**, *64*, 7528-7536.

[33] Laufersweler, M. J.; Rohde, J. M.; Chaumette, J.-L.; Sarazin, D.; Parquette, J. R. *J. Org. Chem.* **2001**, *66*, 6440-6452.

[34] Vötgle, F.; Richardt, G.; Werner, N. *Dendrimer Chemistry*, Wiley-VCH: Weinheim, **2009**, pp. 97-102, and references therein.

[35] Ballauff, M.; Likos, C. N. *Angew. Chem. Int. Ed*. **2004**, *43*, 2998-3020.

[36] Mattice, W. L.; *Dendritic Molecules: Concepts, Syntheses, Perspectives;* Newkome, G. R.; Moorefield, C. N.; Vögtle, F. Eds.; VCH: Weinheim, Germany, **1996**; pp 1-36.

[37] Theodorou, D. N.; Suter, U. W. *Macromolecules* **1985**, *18*, 1206-1214.

[38] (a) Johnson Jr., C. S. *Prog. Nucl. Mag. Res. Sp.* **1999**, *34*, 203-256. (b) Huo, R. Wehrens, R.; van Duynhoven, J. ; Buydens, L. M. C. *Anal. Chim. Acta* **2003**, *490*, 231-251. (c) Li, D.; Keresztes, I.; Hopson, R.; Williard, P. G. *Acc. Chem. Res.* **2009**, *42*, 270-280.

[39] Shi, Z.; Debenedetti, P. G.; Stillinger, F. H. *J. Chem. Phys.* **2013**, *138*, 12A526.

---

[40] Zuccaccia, D.; Macchioni, A. *Organometallics* **2005**, *24*, 3476-3486.

[41] (a) Shou, M.; Mei, Q.; Ettore Jr., M. W.; Dai, R.; Baillie, T. A.; Rushmore, T. H. *Biochem. J.* **1999**, *340*, 845-653. (b) Arnold, S.; Kadenbach, B. *Eur. J. Biochem*. **1997**, *249*, 350-354. (c) Connick, J. P.; Reed, J. R.; Cheng, D.; Cawley, G. F.; Backes, W. L. *FASEB J*. **2012**, *26*, 850-855.

[42] (a) Putzeys, P.; Reijnaers, H. *Nature* **1966**, *212*, 506. (b) Cabrales, Y.; Lores, M.; Machado, Y. *Applied Magnetic Res*onance **2008**, *33*, 207-212. (c) Yuan, Y.; Tam, M. F.; Simplaceanu, V.; Ho, C. *Chem. Rev*. **2015**, *115*, 1702-1724.

[43] Singh, K.; Sharma, A.; Behal, S.; Kaur, P. *Lett. Org. Chem*. **2007**, *4*, 374-377.

[44] Datta-Gupta, N.; Malakar, D.; Rice, L.; Rivers, S. *J. Heteterocyclic Chem*. **1987**, *24*, 629-632.

[45] Matos, M. S.; Hofkens, J.; Verheijen, W.; de Schryver, F. C.; Hecht, S.; Pollak, K. W.; Fréchet, J. M. J.; Forier, B.; Dehaen, W. *Macromolecules* **2000**, *33*, 2967-2973.

[46] Kadish, K. M.; Morrison, M. M.; Constant, L. A.; Dickens, L.; Davis, D. G. *J. Am. Chem. Soc*. **1976**, *98*, 8387-8390.

[47] Allinger, N. L. *Molecular Structure. Understanding Steric and Electronic Effects from Molecular Mechanics*; Wiley: Hoboken, NJ, **2010**.

[48] (a) Haile, J. *Molecular Dynamics Simulations*; Wiley: New York, NY, **1992**; (b) Cramer, C. J. *Essentials of Computational Chemistry*; Wiley: Chichester, UK, **2002**; pp. 63-94 and references therein.

[49] (a) MacroModel, Version 9.9; Schrodinger LLC, New York, NY, **2012**; (b) Mohamadi, F.; Richards, N. G. J.; Guida, W. C.; Liskamp, R.; Lipton, M.; Caulfield, C.; Chang, G.; Hendrickson, T.; Still, W. C. *J. Comput. Chem*. **1990**, *11*, 440-467.

[50] Ryckaert, J. P.; Ciccotti, G.; Berendsen, H. J. C. *J. Comput. Phys*. **1977**, *23*, 327-341.

[51] (a) Naidoo, K. J.; Hughes, S. J.; Moss, J. R. *Macromolecules* **1999**, *32*, 331-341; (b) Teobaldi, G.; Zerbetto, F. *J. Am. Chem. Soc.* **2003**, *125*, 7388-7393; (c) Karatasos, K.; Adolf, D. B.; Davies, G. R. *J. Chem. Phys.* **2001**, *115*, 5310-5318; (d) Lee, I.; Athey, B. D.; Wetzel, A. W.; Meixner, W.; Baker, Jr., J. R. *Macromolecules* **2002**, *35*, 4510-4520.

[52] Field, M. J. *A Practical Introduction to the Simulation of Molecular Systems*; Cambridge University Press: Cambridge, UK, **1999**.

---

[53] Banks, J. L.; Beard, H. S.; Cao, Y.; Cho, A. E.; Damm, W.; Farid, R.; Felts, A. K.; Halgren, T. A.; Mainz, D. T.; Maple, J. R.; Murphy, R.; Philipp, D. M.; Repasky, M. P.; Zhang, L. Y.; Berne, B. J.; Friesner, R. A.; Gallicchio, E.; Levy, R. M. *J. Comput. Chem.* **2005**, *26*, 1752-1780.

[54] Desmond Molecular Dynamics System, version 4.1, D. E. Shaw Research, New York, NY, 2015. Maestro-Desmond Interoperability Tools, Version 4.1, Schrödinger LLC: New York, NY, **2015**.